Designs and High Power Tests of Distributed Coupling Linacs

Mamdouh Nasr, C. Limborg, P. Borchard, Z. Li, S. Tantawi

International Workshop on Breakdown Science and High Gradient Technology

IFIC, 13-16 June 2017, Valencia, Spain

U.S. DEPARTMENT OF ENERGY Office of Science

Stanford ENGINEERING Electrical Engineering

SLAC NATIONAL ACCELERATOR LABORATORY

Outline

- Motivation
- Novel distributed coupling to each accelerator cell enables doubling RF to beam efficiency and ultra-high-gradient operation
- Experimental setup, processing software development and initial results
- The extension of this work to novel dual-mode dual-frequency linac
- Conclusion

This work is motivated by the discovery of the correlation between breakdown rates and the peak magnetic field on surface

Physics of Breakdowns

Discovery of Magnetic Field's Role in Breakdown Triggered New Research Initiative

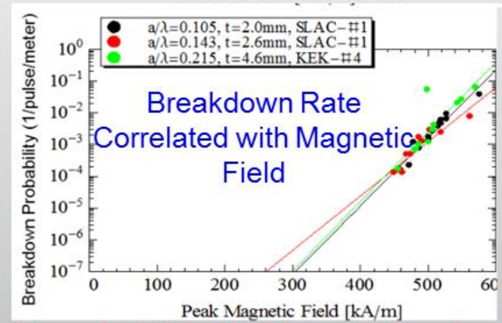

Achieved through studies of surface electric and magnetic fields, processing techniques, surface finish

Material Science

Investigate Materials to Improve the Performance of High Gradient Accelerating Structures

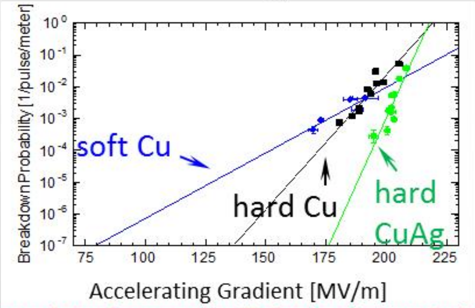

- Enhanced performance with increasing material strength
- Low temperature operation also increases the strength of materials

Innovative Electrodynamics

Geometry of Accelerating Structures Optimized Accounting for:

1. **Our New Understanding of the Physics of Breakdown (magnetic fields, materials etc.)**
2. **The Beam Parameters Required for a Specific Application**

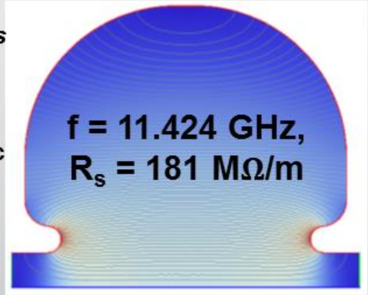

Geometry optimizations for accelerator structures based on reduction of the magnetic surface field

Manufacturing Engineering

Manufacturing Techniques that are Compatible with Superior Materials and Unique Geometries

- Low temperature assembly with clamped structures and welding
- Split-block machining for increased flexibility in fabricating advanced structures and reducing cost

Novel split-block assembly

New linac architecture has to allow for the use of single-cell optimized geometries and compatible with manufacturing techniques that don't require brazing or diffusion bonding

Distributed Coupling: How does it work?

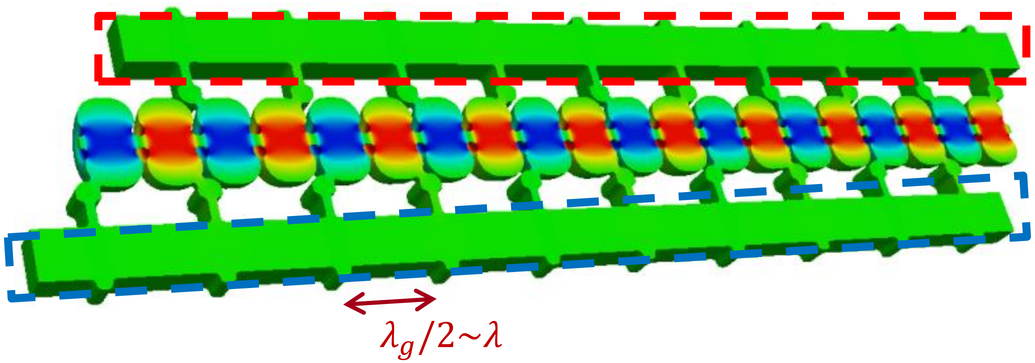

Alternating pairs of cell sections are connected to opposite distribution waveguide manifolds

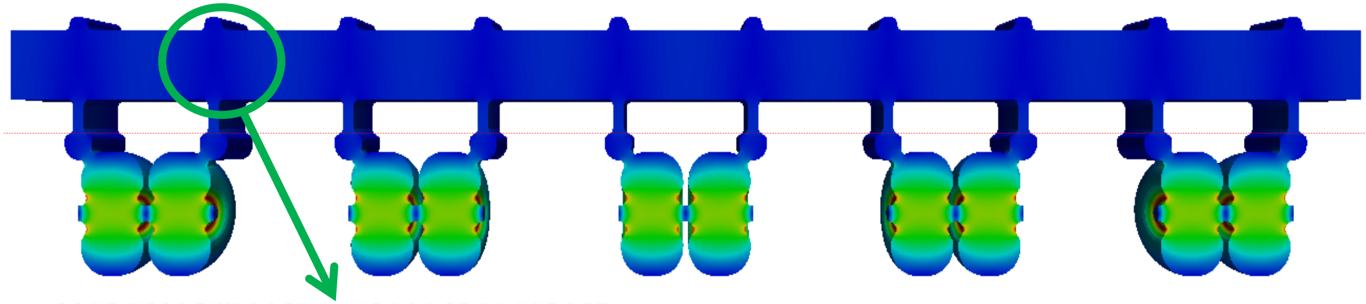

Two separate systems

In-between pure traveling wave

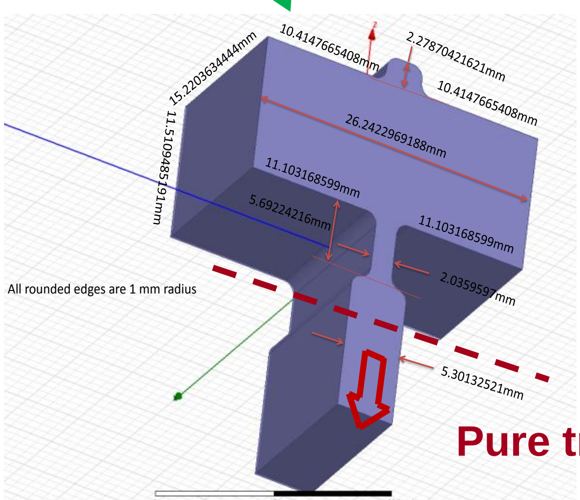

Pure travelling wave

$$S = \begin{pmatrix} \frac{1}{-1-2n} & -1+\frac{1}{1+2n} & -\frac{2e^{i\sigma}\sqrt{n}}{1+2n} \\ -1+\frac{1}{1+2n} & \frac{1}{-1-2n} & \frac{2e^{i\sigma}\sqrt{n}}{1+2n} \\ -\frac{2e^{i\sigma}\sqrt{n}}{1+2n} & \frac{2e^{i\sigma}\sqrt{n}}{1+2n} & e^{2i\sigma}\left(-1+\frac{2}{1+2n}\right) \end{pmatrix},$$

Large isolation between the manifolds and the cavities

S. Tantawi, P. Borchard, Z. Li

Cavities can be optimized without the usual coupling constraints leading to a much enhanced performance

- Cavities can be optimized without the constraint usually applied from the coupling between adjacent cavities.
- This has the benefit of much more efficient designs that consume less RF power.

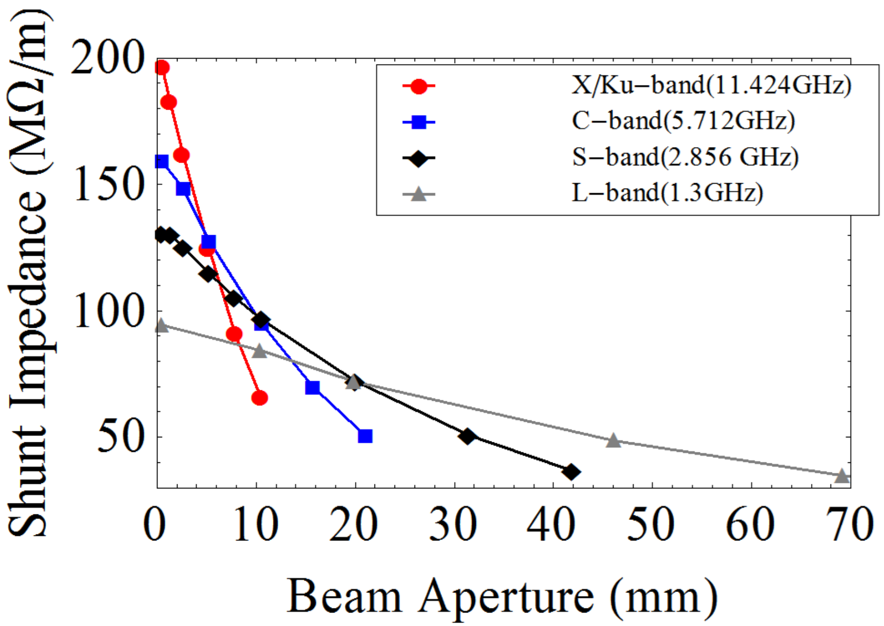

New Scaling Laws Determine the Best Performance for Accelerating Structures

Scalable technology with enhanced shunt impedance capable of reaching high duty factors

S. Tantawi

X-band Distributed Feeding Linac

Under testing at NLCTA: X-band (11.4 GHz), π-mode, 20 cells Linac

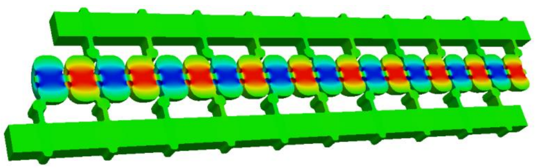

Distributed Coupling to Each Cell

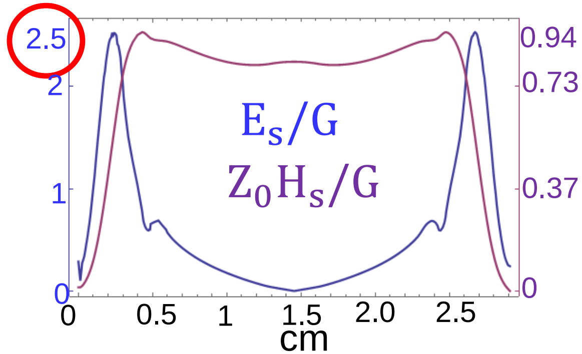

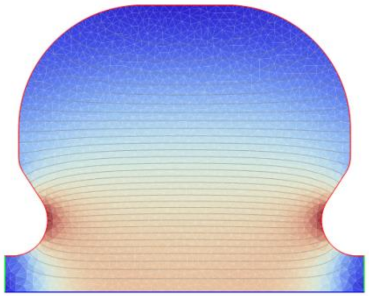

Designed to minimize surface magnetic field

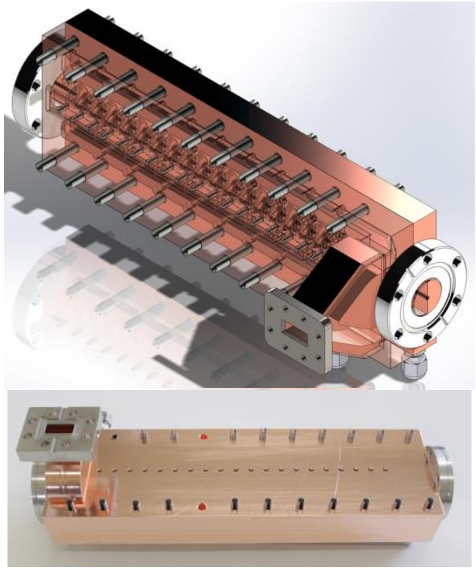

Inexpensive manufacturing using two quasi-identical parts

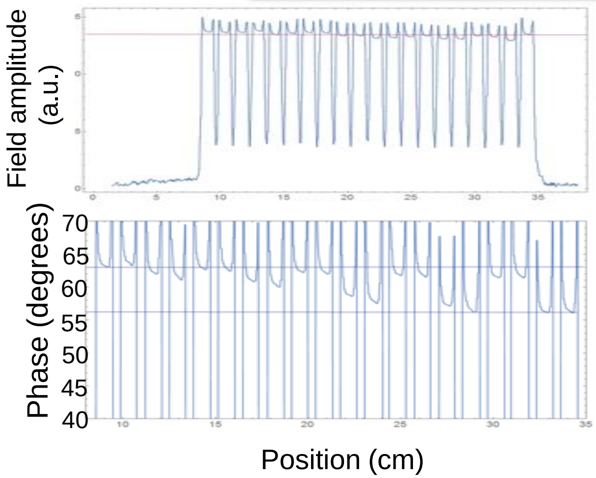

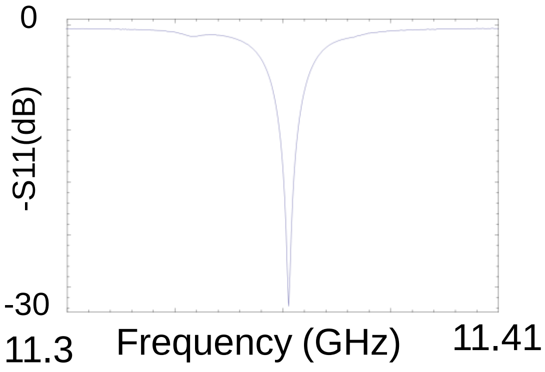

Easy tuning and Single frequency rather than the traditional 20 resonances

Only possible through modern virtual prototyping using high power computing

Experimental setup for processing and testing breakdown rate of this SW structure

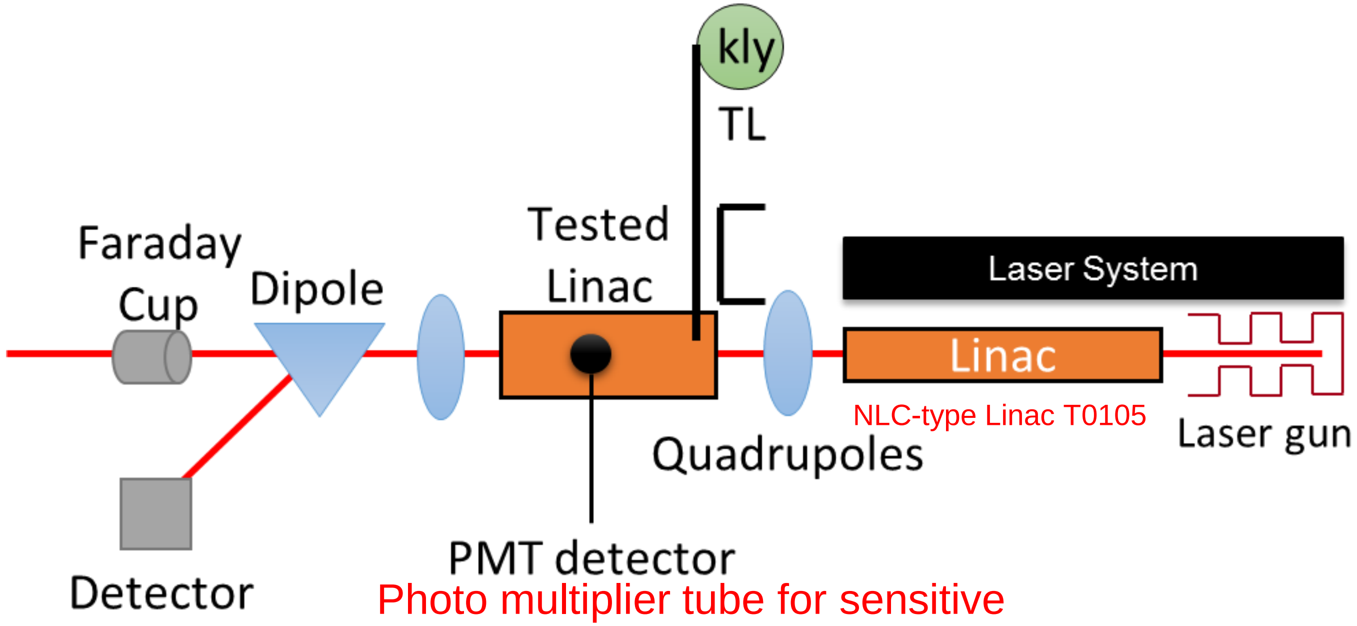

Photo multiplier tube for sensitive detection of dark current

Phosphorus screen to analyze the beam energy

Experimental setup for processing and testing breakdown rate of this SW structure

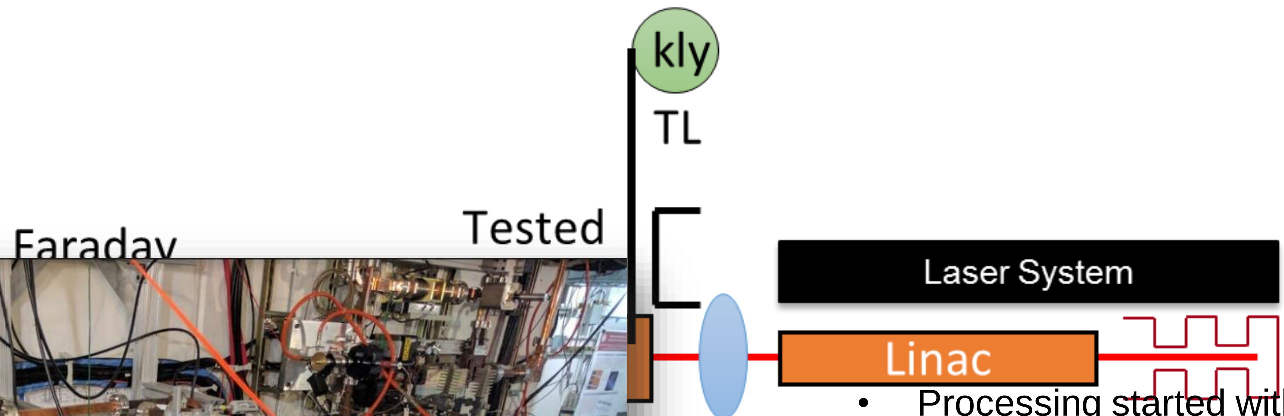

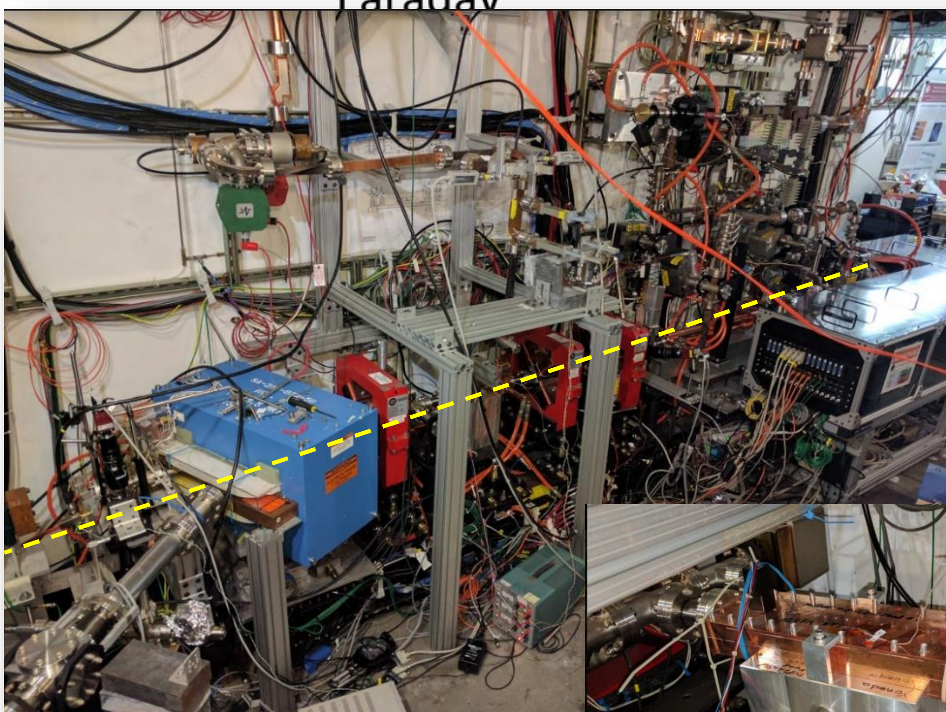

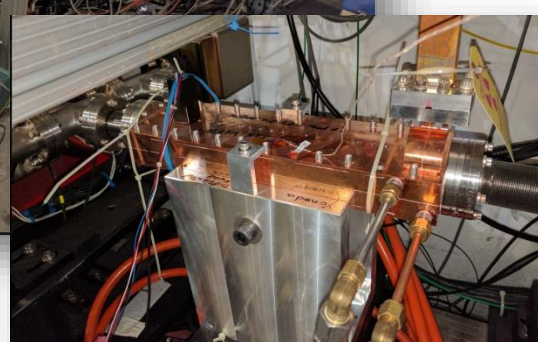

- Processing started with a single klystron and 300 ns square pulses and we reached a peak gradient of 130 MV/m, limited by the available klystron power.
- Then, using stepped pulses for a flat gradient of 150 ns we reached a maximum gradient of 100 MV/m , limited by the available klystron power.

- Total processing with klystron alone of 150 hours at 60 Hz.

- We decided to install a pulse compressor (SLED line).

Experimental setup for processing and testing breakdown rate of this SW structure

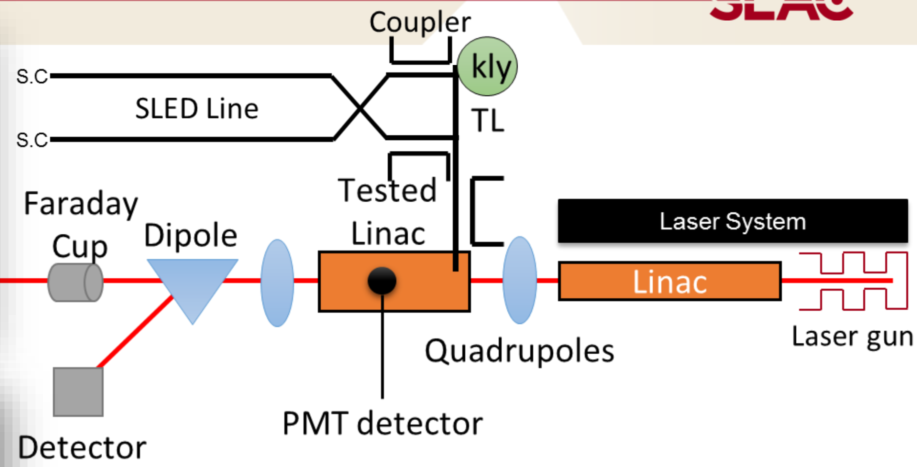

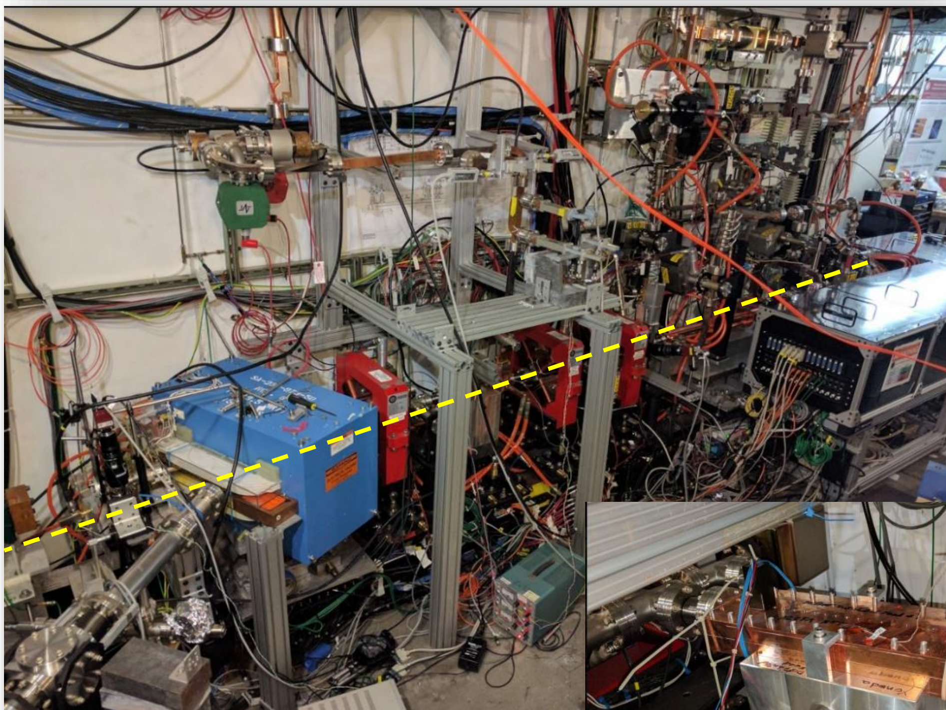

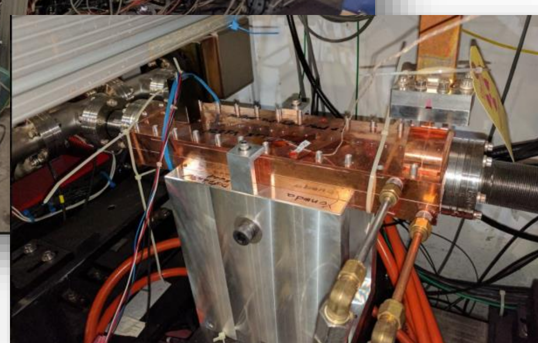

Experimental setup for processing and testing breakdown rate of this SW structure

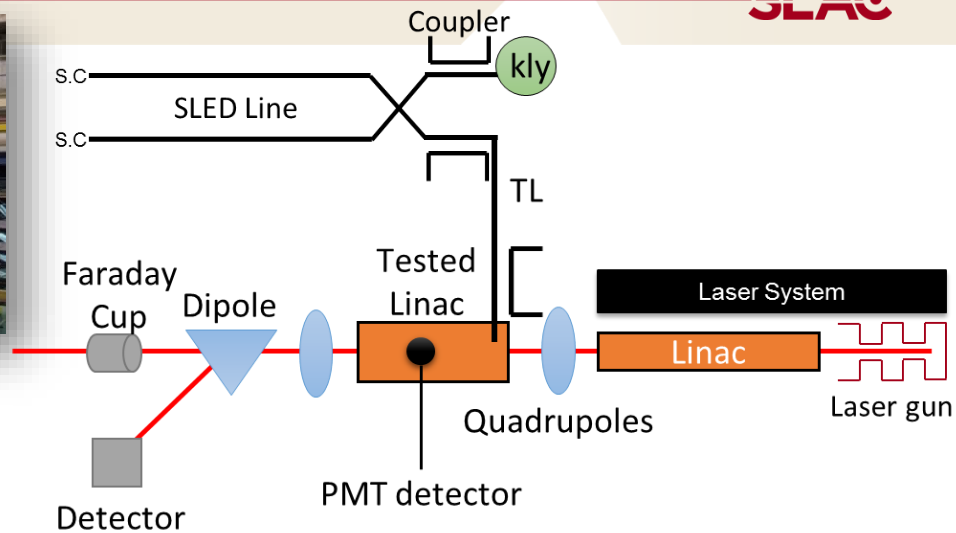

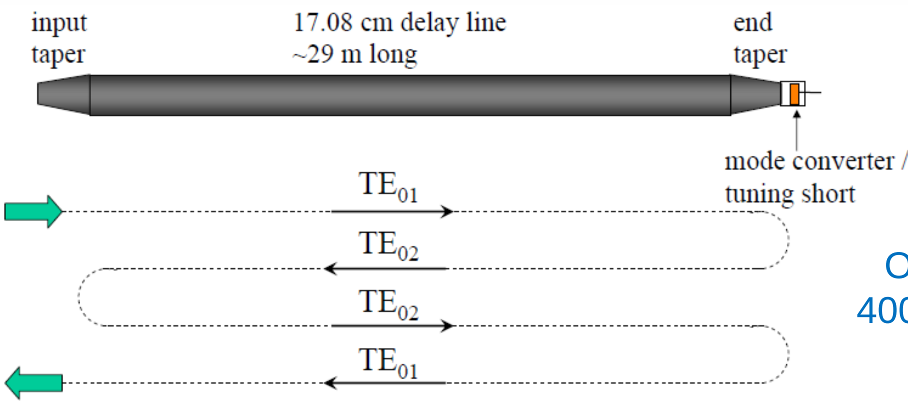

ON
400 ns

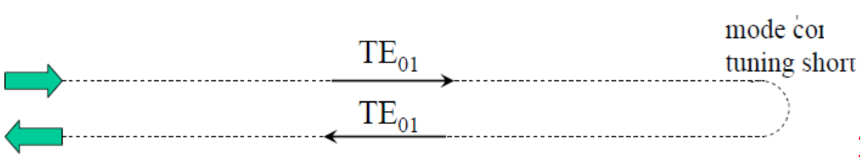

OFF
200 ns

Tantawi, S. G. et al. High-power multimode X-band rf pulse compression system for future linear colliders. Phys. Rev. ST Accel. Beams 8, 042002 (2005).

Experimental setup for processing and testing breakdown rate of this SW structure

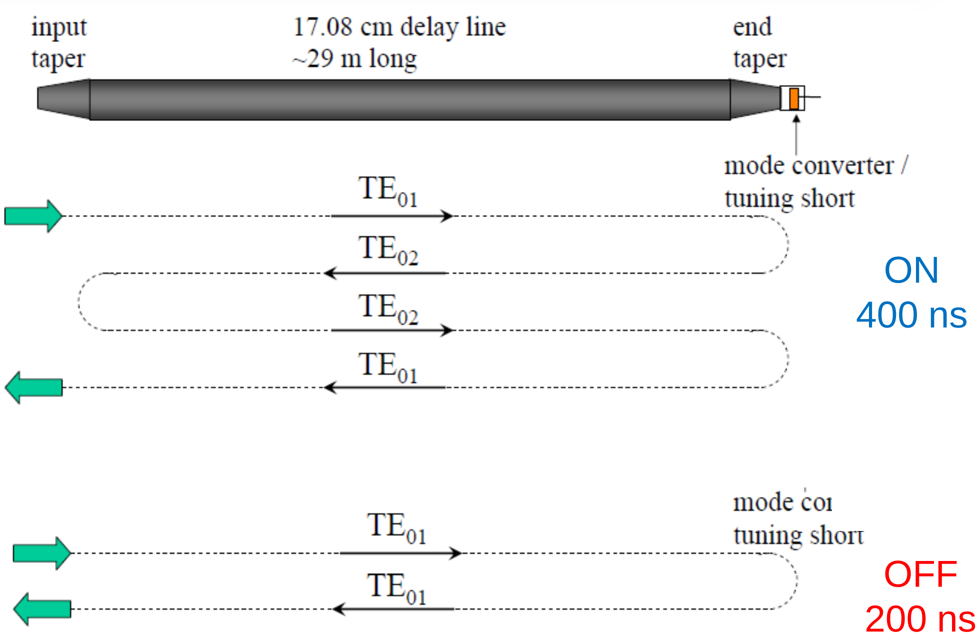

Square pulse: Mode Converter ON

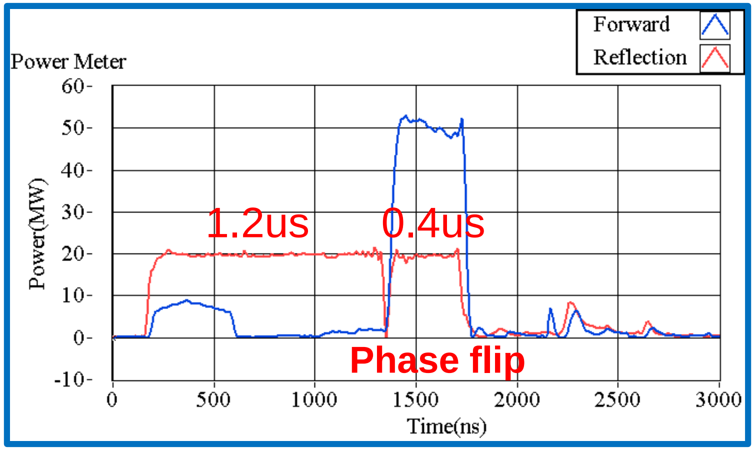

Stepped pulse: Mode Converter OFF

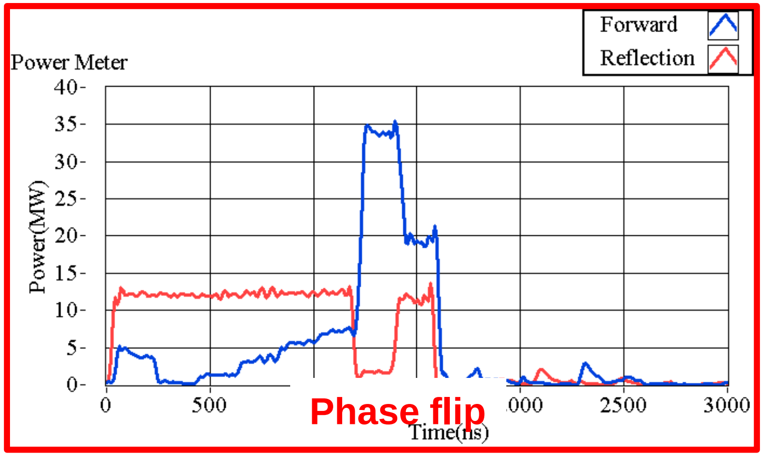

Tantawi, S. G. et al. High-power multimode X-band rf pulse compression system for future linear colliders. Phys. Rev. ST Accel. Beams 8, 042002 (2005).

Developments of processing algorithm software

- Demodulation
- Pulse Correction
- Cavity model fitting
- Gradient Calculation
- Processing Code

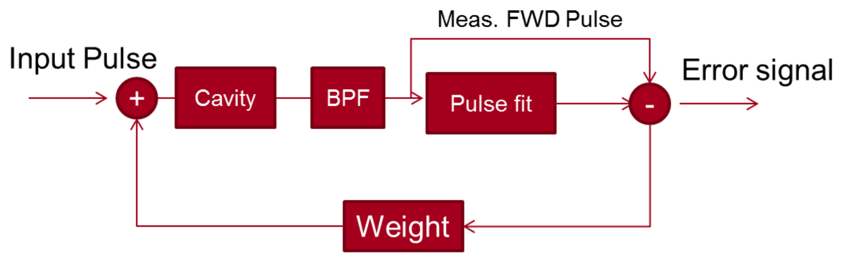

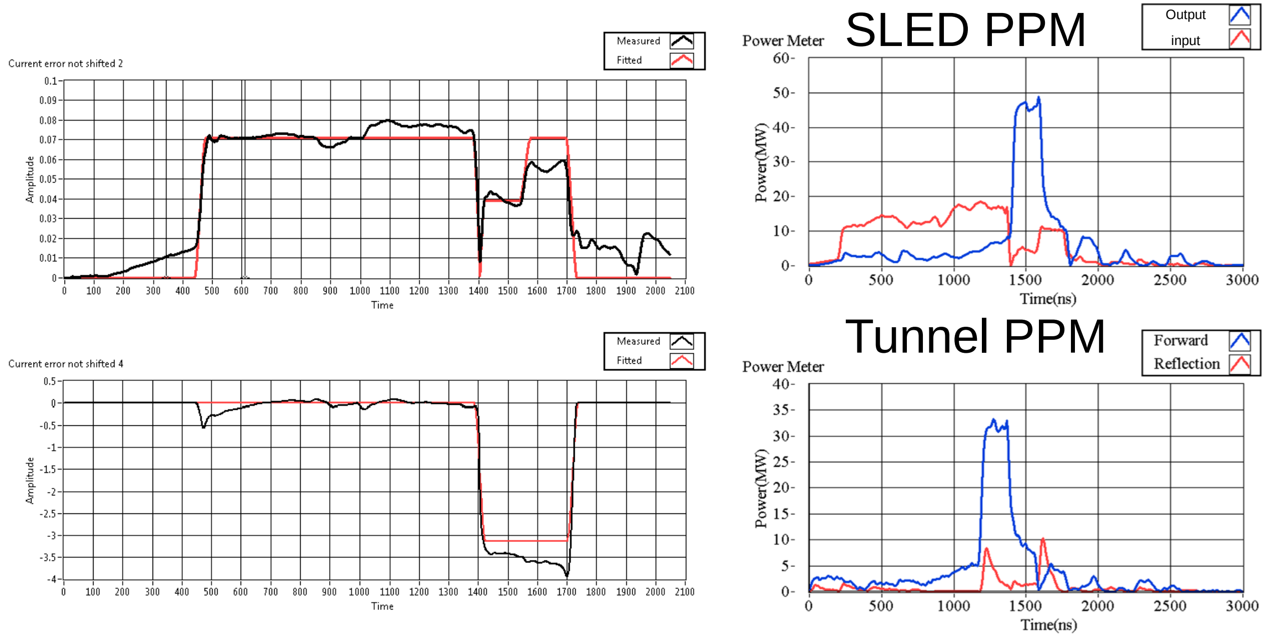

M. Nasr, S. Tantawi

Processing software Developments

- Demodulation
- Pulse Correction
- Cavity model fitting
- Gradient Calculation
- Processing Code

$$\Gamma(\omega) = \frac{\Gamma_0 + jQ_t\delta}{1 + jQ_t\delta}, \delta = \frac{\omega}{\omega_0} - \frac{\omega_0}{\omega}$$

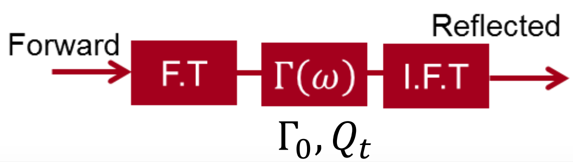

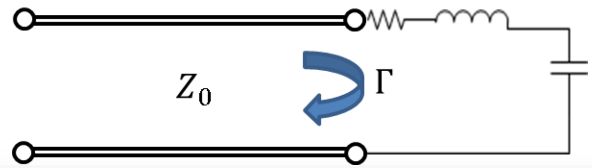

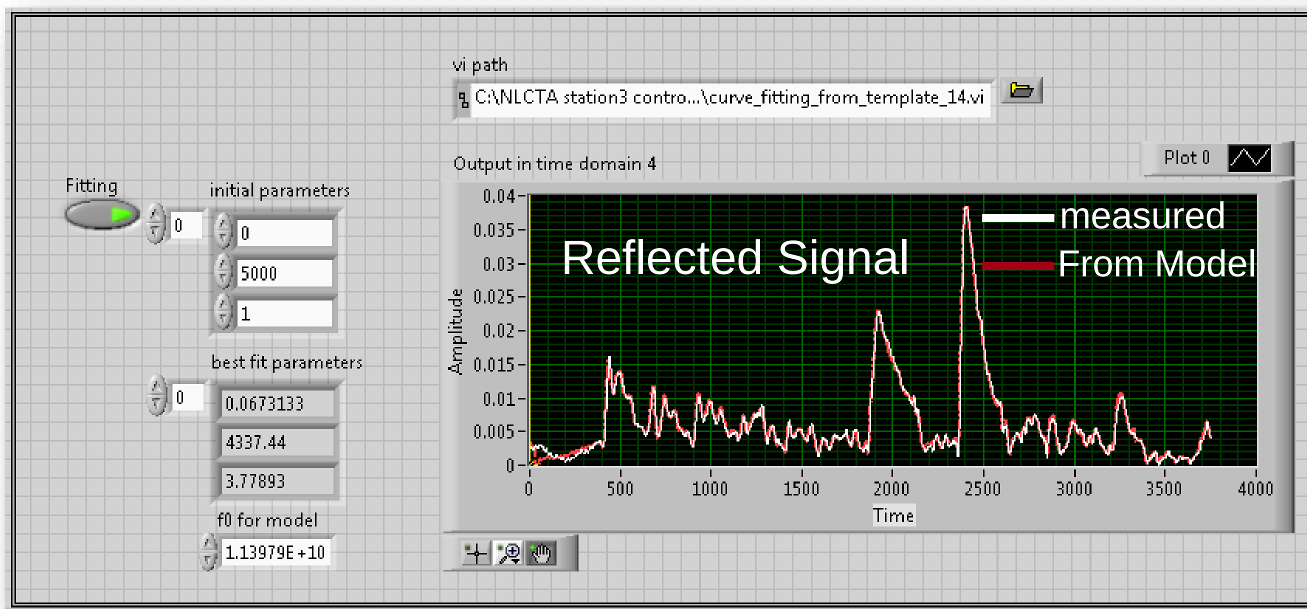

M. Nasr, S. Tantawi

Processing software Developments

Demodulation

Pulse Correction

Cavity model fitting

Gradient Calculation

Processing Code

$$\Gamma(\omega) = \frac{\Gamma_0 + jQ_t\delta}{1 + jQ_t\delta}, \delta = \frac{\omega}{\omega_0} - \frac{\omega_0}{\omega}$$

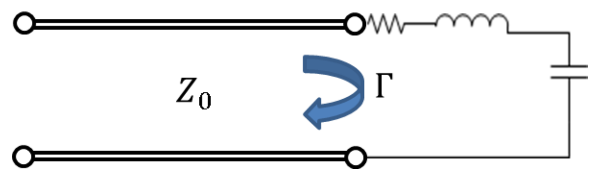

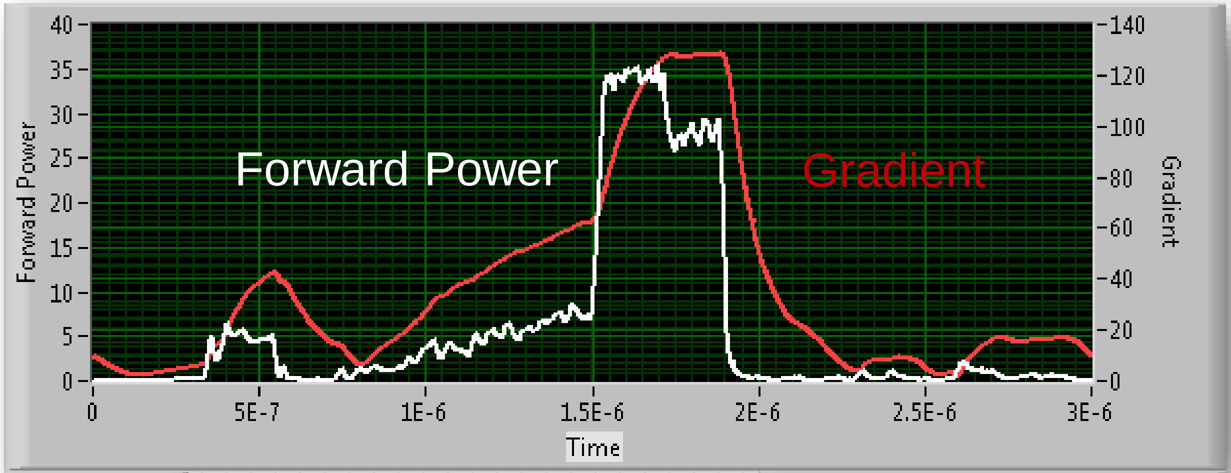

M. Nasr, S. Tantawi

Processing software Developments

SLAC

Demodulation

Pulse Correction

Cavity model fitting

Gradient Calculation

Processing Code

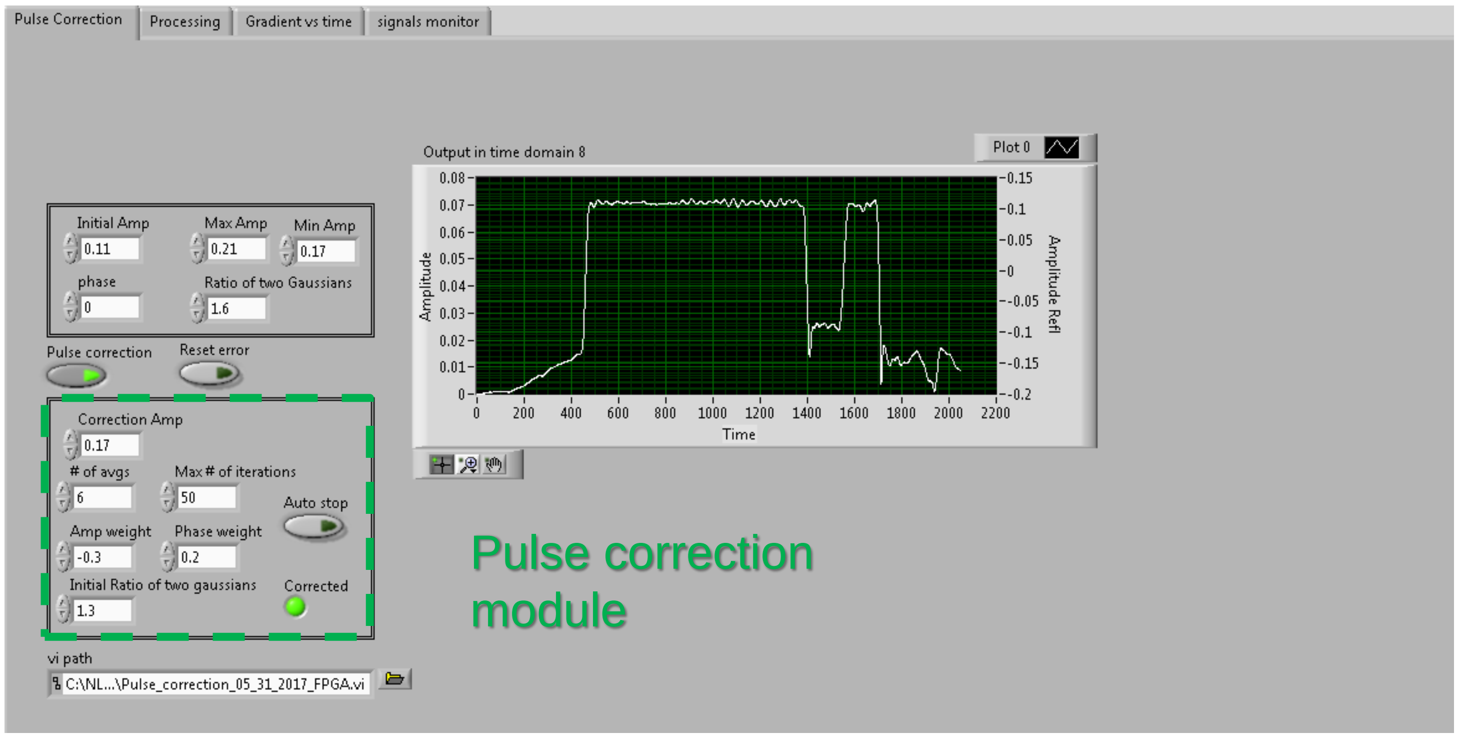

M. Nasr, S. Tantawi

Processing software Developments

Demodulation

Pulse Correction

Cavity model fitting

Gradient Calculation

Processing Code

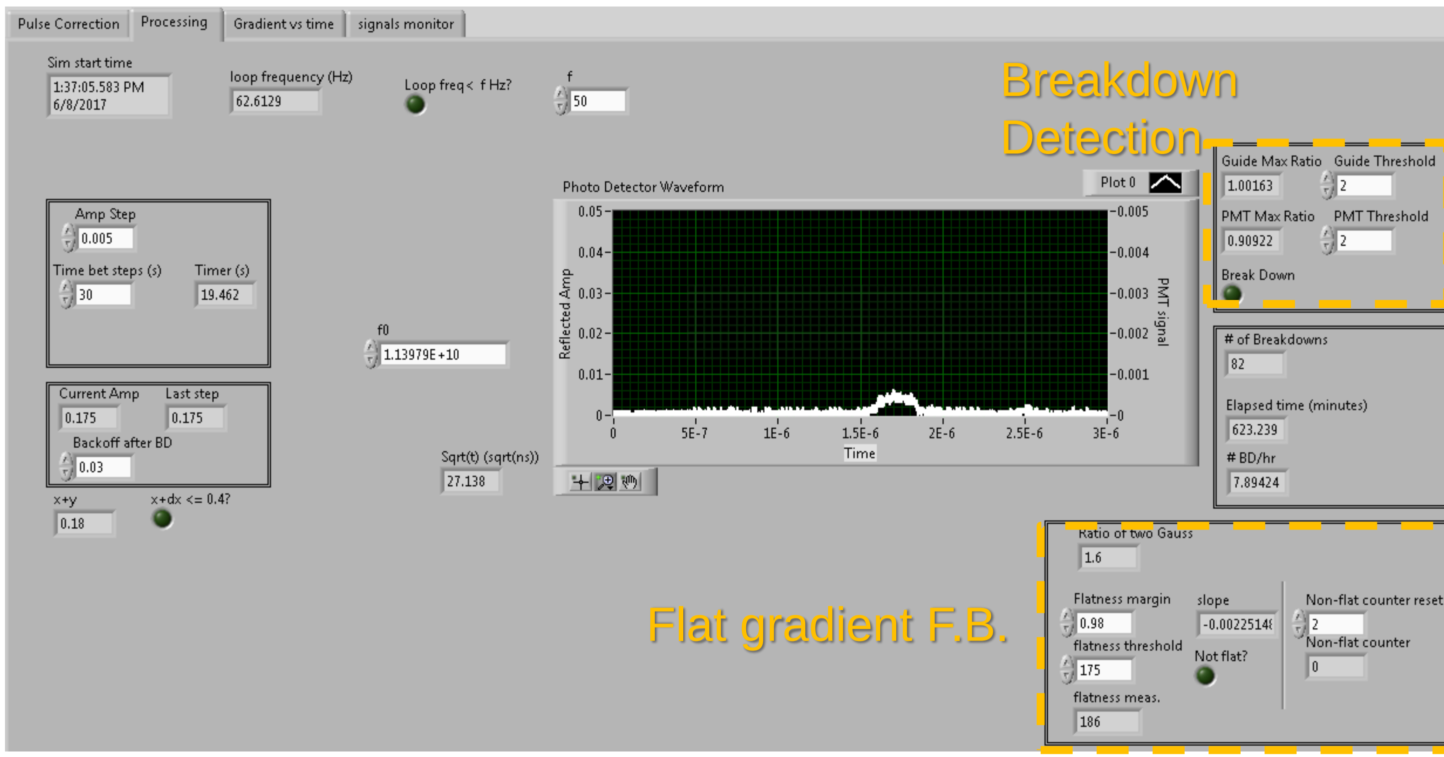

M. Nasr, S. Tantawi

Processing software Developments

Demodulation

Pulse Correction

Cavity model fitting

Gradient Calculation

Processing Code

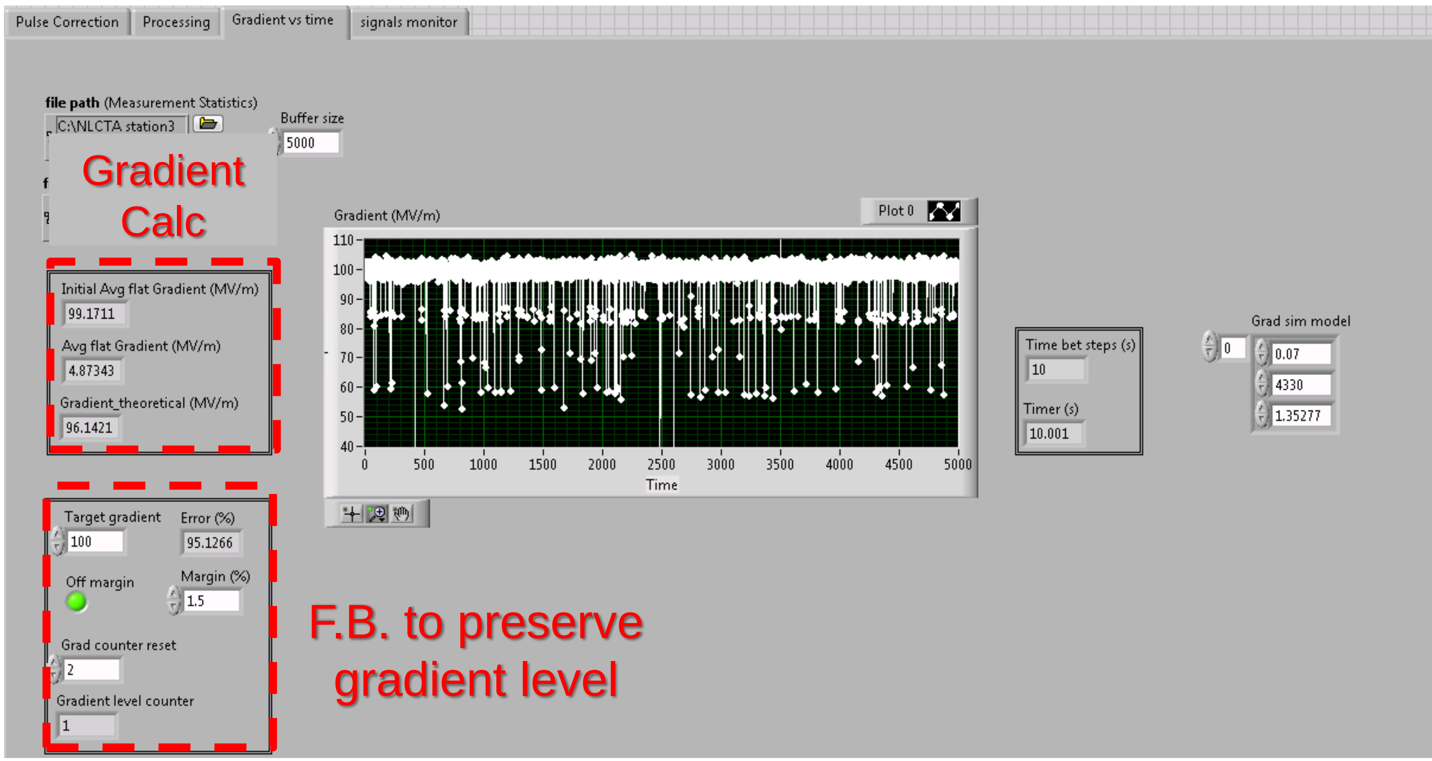

M. Nasr, S. Tantawi

Verification of high shunt impedance and acceleration properties of the structure

- Operating with ~100 MeV/m gradient with 16.5 MW of input power and 300 ns square pulse **before installation of the SLED line**
- Confirmation of gradient by measuring 24 MeV energy gain
- Confirmation of RF performance by measuring wakefield power to determine charge

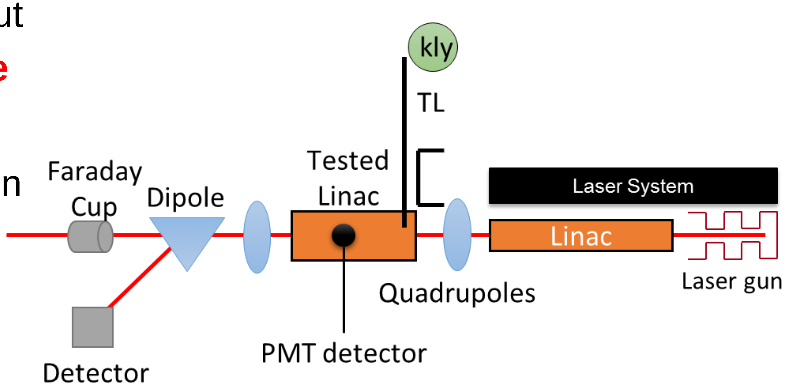

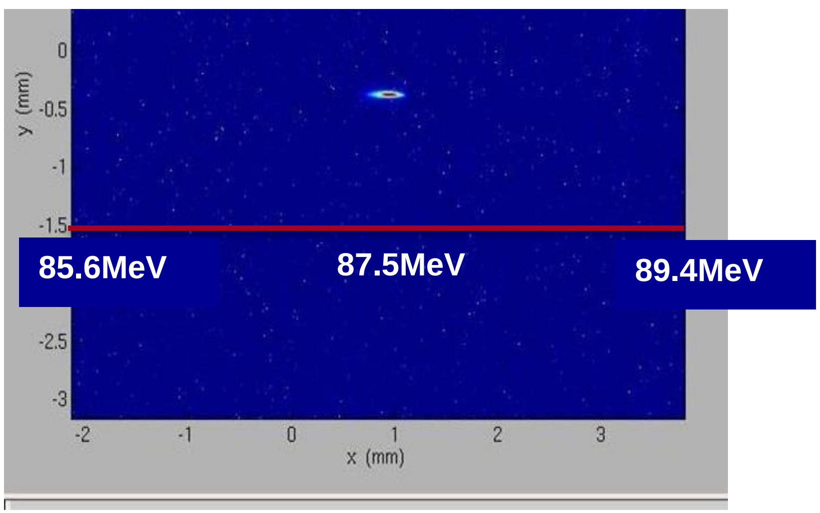

Beam Energy

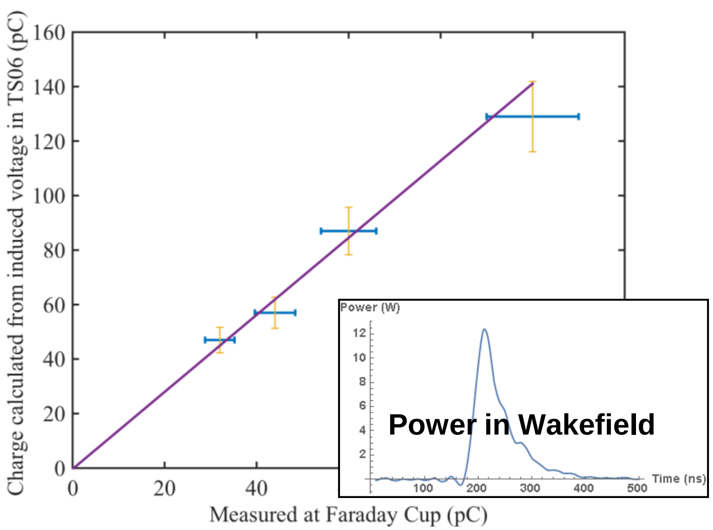

Measured Charge with Faraday Cup and Calculated from Induced Wakefield

M. Nasr , C. Limborg, S. Tantawi

Verification of high shunt impedance and acceleration properties of the structure

After SLED line installation

- Charges drifted and accelerated from the first cell have energy gain ~ Gradient / 4
- Confirmation was done at ~140 MV/m gradient by measuring 35.7 MeV maximum dark current energy

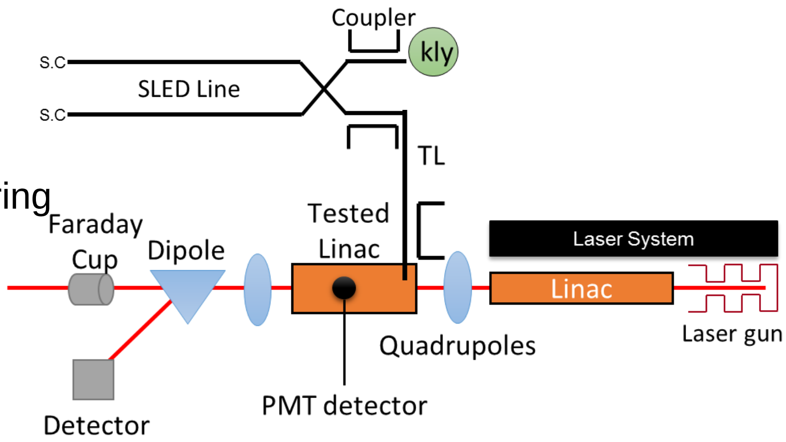

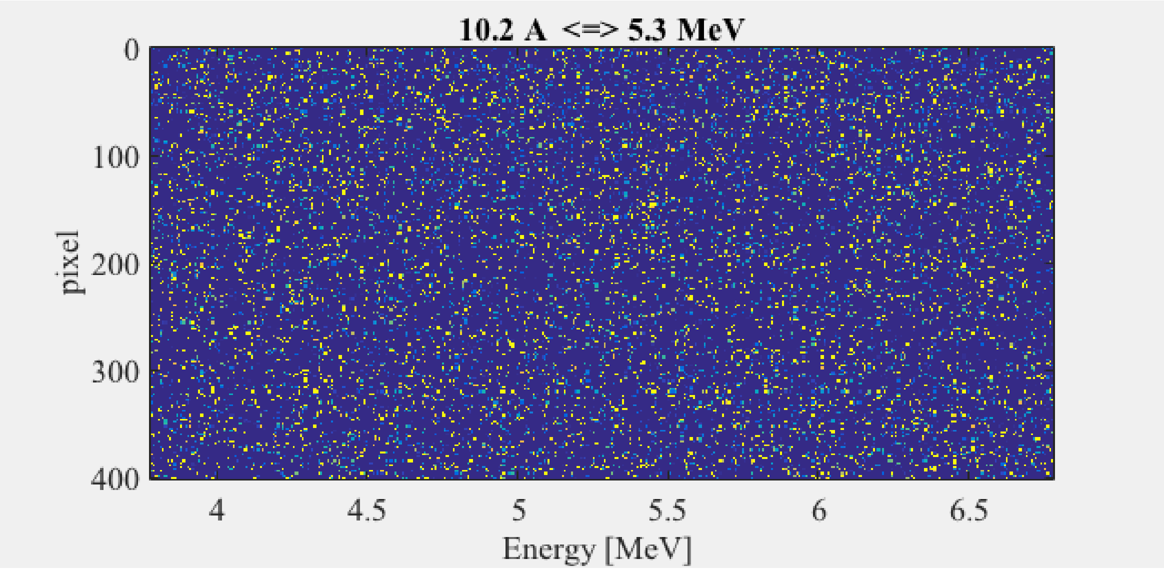

Measured dark current energy

M. Nasr , C. Limborg, S. Tantawi

Fowler-Nordheim field enhancement factor

- After connecting the SLED system and working with the stepped pulse, we had ~100 processing hours at 60 Hz

$$\frac{\mathrm{Max}[E_s]}{G} = 2.5$$

- Fowler-Nordheim field enhancement factor is calculated using the measured charge at the Faraday cup and fitting the data

This is to be verified

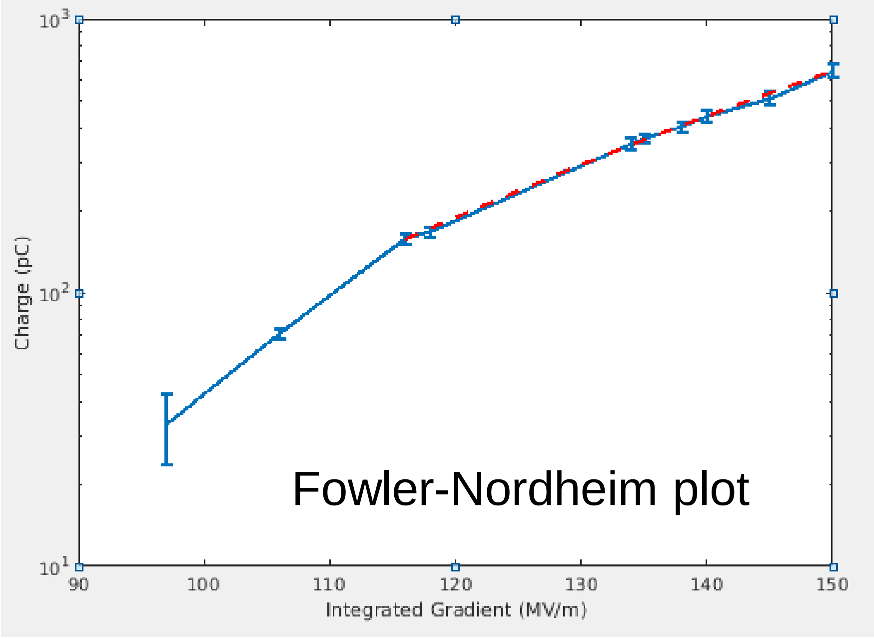

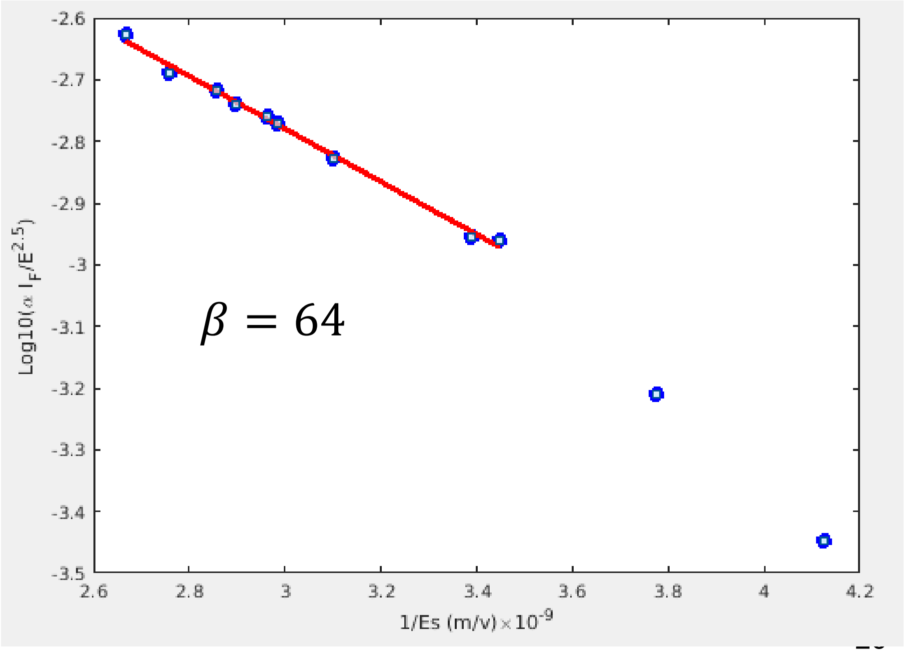

M. Nasr , C. Limborg, S. Tantawi

Outline

- Motivation
- Novel distributed coupling to each accelerator cell enables doubling RF to beam efficiency and ultra-high-gradient operation
- Experimental setup, processing software development and initial results
- The extension of this work to novel dual-mode dual-frequency linac
- Conclusion

Having every cell fed individually by a manifold naturally inspires the use of another manifold with another mode feeding the same cavity

SLAC

- Typically power ∝ $(\text{gradient})^2$
- Performance of cavity improves when powered with two different RF modes
  - **Efficiency:** Linear superposition of fields by adding power in the two modes.
  - **Gradient:** doubling the accelerating gradient without doubling surface fields; ~ 300 MV/m gradient at room temp

Previous designs were strict to harmonically relate frequencies which is not optimal.

Our design is free from this constraint, and instead operate at the common sub-harmonic of the used frequencies.

Using distributed feeding network that feeds every cell independently for each mode.

M. Nasr et al. A Novel Dual-Mode Dual-Frequency Linac Design, IPAC,17

Conceptual Foundation for Dual-Mode Operation

The total energy gain (ΔU) for a charged particle with a charge (e) that passes through a cavity of length (L) and operating simultaneously with two modes can be expressed as

$$\Delta U = e\int_0^L [\mathcal{E}_1(z,t) + \mathcal{E}_2(z,t)]dz = e(G_1 + G_2)L = eG_{tot}L$$

$$\therefore G_{tot}^2 = (G_1 + G_2)^2 = r_1P_1 + r_2P_2 + 2\sqrt{r_1r_2P_1P_2}$$

$$\therefore r_t = \frac{G_{tot}^2}{P_{L,tot}} = \frac{r_1 + \alpha r_2 + 2\sqrt{\alpha r_1 r_2}}{1+\alpha}, \alpha = \frac{P_{L,2}}{P_{L,1}}$$

Deriving the condition for maximum shunt impedance

$$\frac{\partial r_t}{\partial \alpha} = 0$$

$$\vdots$$

Maximum: $\alpha = \frac{r_2}{r_1} \rightarrow r_{tot} = r_1 + r_2$ ➡

$$\frac{G_2}{G_1} = \frac{\sqrt{r_2P_{L,2}}}{\sqrt{r_1P_{L,1}}} = \frac{r_2}{r_1}$$

M. Nasr et al. A Novel Dual-Mode Dual-Frequency Linac Design, IPAC,17

Conceptual Foundation for Dual-Mode Operation

SLAC

The maximum total shunt impedance for dual-mode operation equals to the summation of the individual shunt impedance for each mode.

Under the constraint that the gradient (power) ratio of the two modes equals to the individual shunt impedance ratio.

The derivation didn't require any harmonic relation between the operating frequencies.

M. Nasr et al. A Novel Dual-Mode Dual-Frequency Linac Design, IPAC,17

Optimization Results

- We provide two sets of designs that utilize TM_{011} or TM_{020} as the second mode of operation.

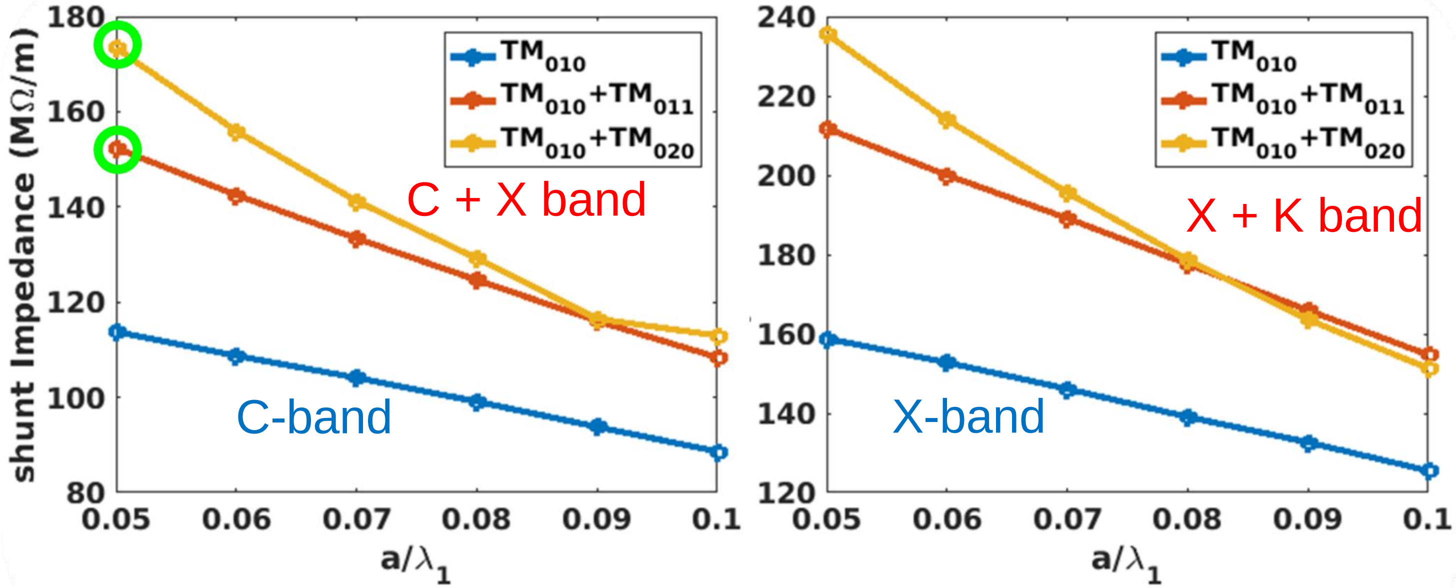

- $\mathrm{TM}_{010} + \mathrm{TM}_{011}$ designs: the cell width $\approx 0.5\lambda_1$ with $f_{res,2} \approx 1.66\, f_{res,1}$
- $\mathrm{TM}_{010} + \mathrm{TM}_{020}$ designs: the cell width $\approx 0.3\lambda_1$ with $f_{res,2} \approx 2.3\, f_{res,1}$

These new dual-mode dual-frequency designs provide much enhanced acceleration efficiency compared to single mode optimized designs

M. Nasr, S. Tantawi

How does the fields add on the surface?

$\mathbf{TM_{010} + TM_{011}}$

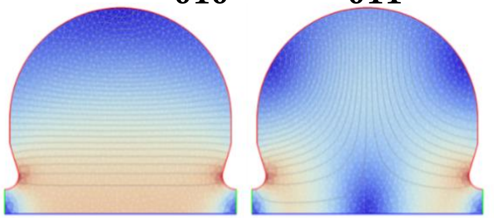

- $Rs_{tot} = 153\ \mathrm{M\Omega/m}$
- $f_{res,1} = 5.712$
- $f_{res,2} = 9.629$ GHz
- $f_{com} = 163.2$ MHz

$\mathbf{TM_{010} + TM_{020}}$

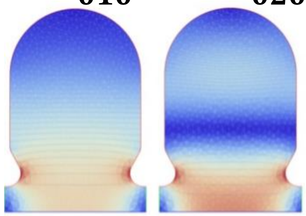

- $Rs_{tot} = 174\ \mathrm{M\Omega/m}$
- $f_{res,1} = 5.712$ GHZ
- $f_{res,2} = 12.95$ GHz
- $f_{com} = 380.8$ MHz

Surface fields plots for each individual mode

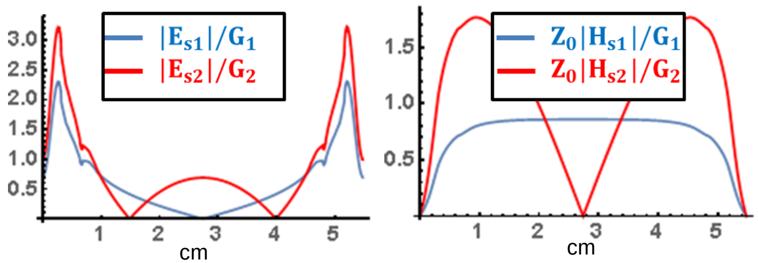

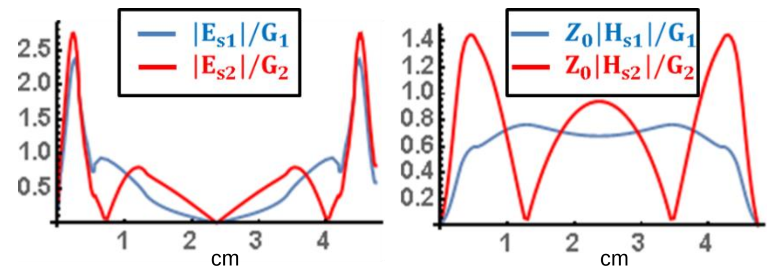

Total surface fields plots at many time instants during a common-harmonic period

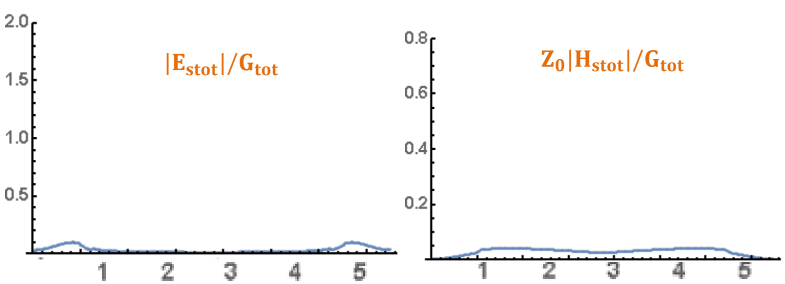

Common-harmonic period=6.13 ns

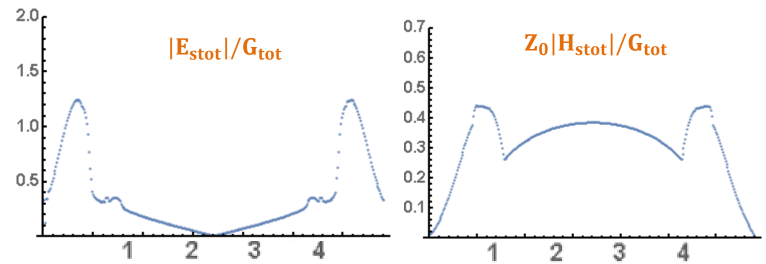

Common-harmonic period=2.63 ns

M. Nasr, S. Tantawi

How does the fields add on the surface?

$\mathbf{TM_{010} + TM_{011}}$

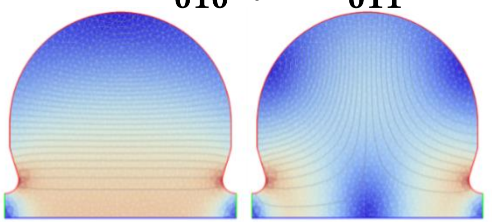

- $Rs_{tot} = 153\ \mathrm{M\Omega/m}$
- $f_{res,1} = 5.712$
- $f_{res,2} = 9.629$ GHz
- $f_{com} = 163.2$ MHz

$\mathbf{TM_{010} + TM_{020}}$

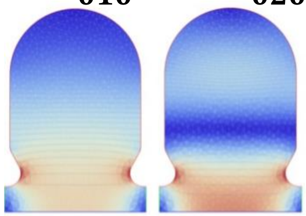

- $Rs_{tot} = 174\ \mathrm{M\Omega/m}$
- $f_{res,1} = 5.712$ GHZ
- $f_{res,2} = 12.95$ GHz
- $f_{com} = 380.8$ MHz

Surface fields plots for each individual mode

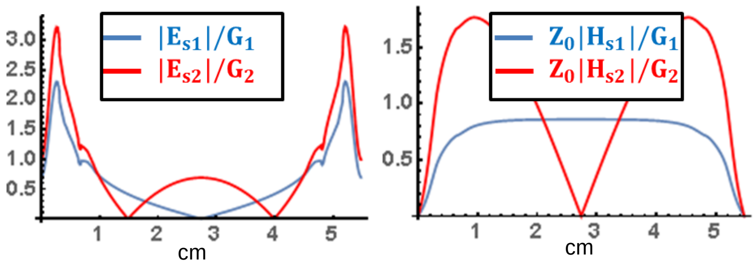

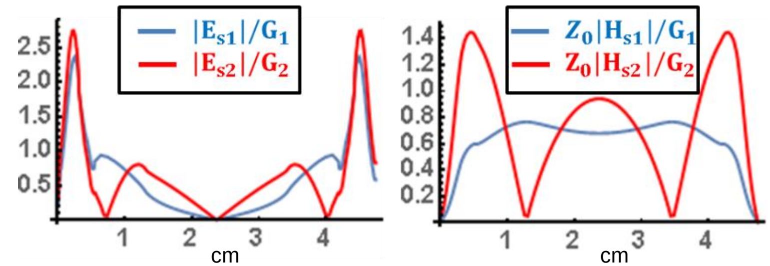

Total surface fields plots at many time instants during a common-harmonic period

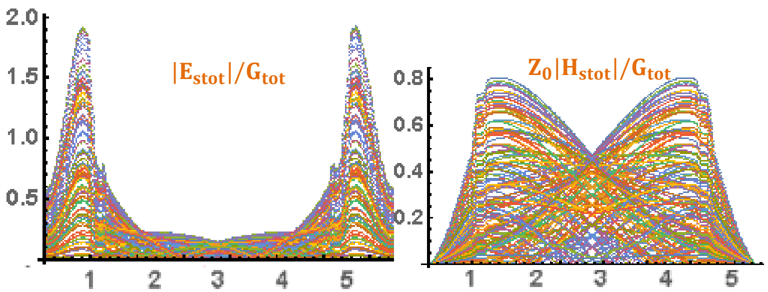

Common-harmonic period=6.13 ns

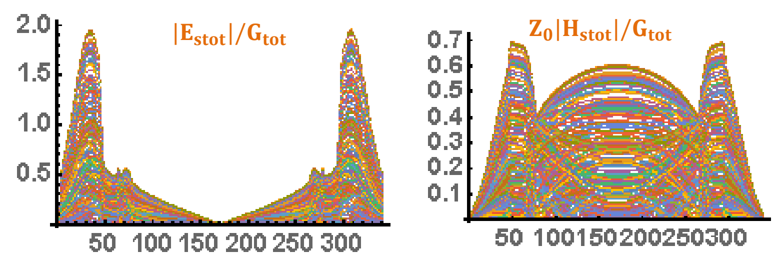

Common-harmonic period=2.63 ns

Maximum fields for the two modes doesn't occur at the same time.
The maximum fields occur over the larger period of the common-harmonic.

Next steps for the dual-mode dual-frequency design

- We are now working on developing more optimized generic shapes to produce even higher performance.

- Also, we are working on the design for the distributed feeding network for our dual-mode designs.

Conclusion

- Distributed coupling Linacs provides a new technology that enables much enhanced cell design optimization and pushes the limitation of Linacs performance.

- An X-band SW distributed feeding Linac is under testing at NLCTA with the experimental setup done and the processing software developed to push the structure to ultra-high gradient.

- The idea of distributed coupling Linac is extended to a novel dual-mode dual-frequency designs. The frequencies are not constrained to be harmonics and the designs provides much enhanced performance and lower surface fields compared to single-mode optimized designs.

Acknowledgement

Sami Tantawi

For all his support and continuous guidance

Cecile Limborg

For being very dedicated and helpful in the experiment at NLCTA

NLCTA team

Michael Dunning, Doug McCormick, Keith Jobe, Carsten Hast

For helping us on daily basis at NLCTA

Colleagues at SLAC

Valery Dolgashev, Muhammed Shumail, Alysson Vrielink, Emilio Nanni, Filippos Toufexis, Alex Cahill

For all their help and the useful discussions

Thanks!